Comparison of Fluid Flow and Heat Transfer for 1D and 2D Models of an In-Line Pulse Tube Refrigerator

K.W. Martin[1,2], C. Dodson[1], A. Razani[3]

[1]Spacecraft Component Thermal Research Group
Kirtland AFB, NM 87117-5776

[2]A-tech Corporation dba Applied Technology Associates aka ATA
Albuquerque, NM 87123

[3]The University of New Mexico
Albuquerque, NM 87131

ABSTRACT

Lower order models are commonly utilized for preliminary designs and optimization of cryocoolers. These models are at most one dimensional and therefore often cannot adequately predict the behaviors of fluid flow and heat transfer in cryocoolers that are inherently multi-dimensional. We simulate a linear pulse tube cryocooler using a two dimensional axisymmetric computational fluid dynamics (CFD) model. We compare the CFD to the results obtained from the SAGE® software normally used in the design and optimization of pulse tube and Stirling cryocoolers. These models are compared using second-law analysis techniques, specifically examining the losses in the pulse tube region. The results from both models are examined and instances where the models disagree are identified.

INTRODUCTION

Pulse tube cryocoolers (PTCs) play an important role in satisfying the need for cryogenic cooling of space-based infrared detectors as well as many other applications requiring coolers with high reliability, low vibration, and high efficiency.[1] Given the highly non-linear nature of the oscillating flow problem found in cryocoolers, engineers rely heavily on simulation to predict cooler behavior and designs for prototype models. Generally, quick first-order models are used, such as Gedeon Associate's Sage, which utilize corrections from experiments. These models closely resemble cooler performance without having to resort to the more time consuming computation fluid dynamics (CFD) simulations. The flow near complicated geometries like junctions (at components with different diameters), flow straighteners and jet blockers are ideal candidates for the usage of CFD simulation. These CFD simulation results are of interest when compared to lower order modeling counterparts. Compared in this paper are the results from parameters obtained in an optimized design paper by Zhang et. al. [2] as simulated in Sage® [3] and results are compared to a 2D axisymmetric model solved by the CFD code built by Ansys Fluent ®. [4] Several investigators have utilized the CFD simulation of oscillatory heat and mass flows for PTRs. [5-11]

Cryocoolers 18, edited by S.D. Miller and R.G. Ross, Jr.

Table 1. Parameters utilized and calculated by the low and high order simulations, including some values from the cooler experiment[2].

Component	Parameter	Value(s)
System level	Reject Temperature	300 K
	Charged Pressure	3.0 MPa
	Working fluid	Helium (ideal)
Compressor (COMP)	Power Consumption	93 W (Sage) / 91 W (CFD)
	Operating Frequency	48 Hz
	Time step size (CFD)	2.60542 microseconds
	Maximum volume Swept (Sage)	8.2 cc
	Stroke length (CFD)	5.6 mm
	Diameter (CFD)	25 mm
Aftercooler (AC)	Diameter x length	20 mm x 5 mm
Regenerator (REG)	Diameter x length	20 mm x 60 mm
	Matrix-stainless steel	400 mesh
	Porous media (CFD)	$\flat$=2.5295e-11, C=1.2e5, porosity=.692
		$\flat_r$=5.348e-12, C_r=240000 (Ref. [7])
	Random Fiber Matrix SS304 (Sage)	D_{wire}= 0.025 mm
Cold Heat Exchanger (CHX)	Diameter x length	20 mm x 5 mm
	No-Load Temperature (Sage)	51 K
	Cooling Capacity	7.7 W (Sage) / 5.1 W (CFD) / 8 W (Exp. Ref. [2])
Same for (AC, CHX, HHX)	Matrix-copper	Woven screen matrix, porosity=.68, D_{wire}= 0.025 mm
Same for (AC, CHX, HHX)	Porous media (CFD)	$\flat$=1.345e-9, C=8147, porosity=.68 (Ref. [7])
	Isothermal wall boundary temperature (CFD)	90 K
Pulse Tube (PT)	Diameter x length	14.9 mm x 71 mm
Hot Heat Exchanger (HHX)	Diameter x length	14.9 mm x 5 mm
Inertance Tube 1 (IT1)	Diameter x length	3 mm x 1.09 m
Inertance Tube 2 (IT1)	Diameter x length	4.5 mm x 3.2 m
Reservoir (RES)	Volume	250 cm^3
	Diameter x length (CFD)	43 mm x 43 mm

CFD AND SAGE SIMULATIONS

We utilized the values shown in Zhang et. al.[2] for both our CFD and Sage simulations. Values not given in the paper were estimated using Sage optimization simulations using Sage's pulse tube modeler and ideal helium for the working fluid. All of these values are shown in Table 1. The compressor swept volume in Sage was adjusted such that both Sage and CFD had similar input powers. The cold head simulated in Sage is shown in Figure 1.

The commercial CFD code Ansys Fluent (version 14.5.7)[4] was used to numerically solve the time dependent mass, momentum, and energy equations for a compressible ideal gas helium working fluid. The compressor piston was modeled as a dynamic mesh that utilized a user-defined function (UDF) to describe the sinusoidal velocity of the piston wall as a function of time. The heat exchangers of the aftercooler, regenerator, cold heat exchanger (HX) and the hot HX were modeled using Fluent's porous media models.[7] Two inertance tubes are modeled and are attached to a fully meshed reservoir. All of the walls are modeled as adiabatic, except for the HXs, which are isothermal. The simulations are run using the unsteady-second order time method that solves the Navier-

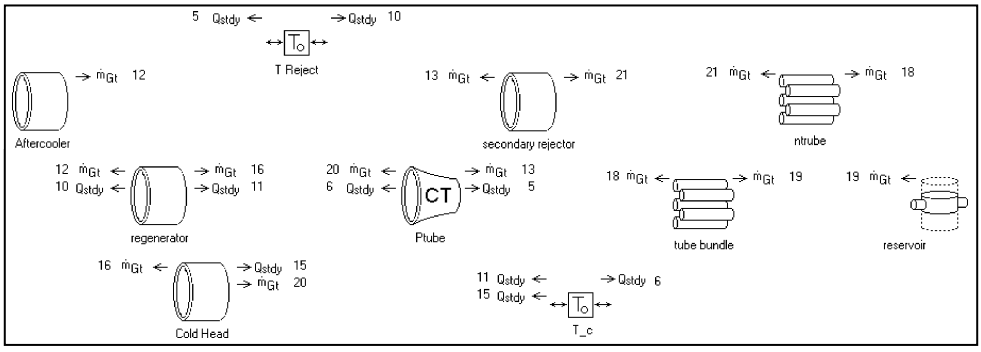

Figure 1. Sage model

Stokes equations utilizing the PRESTO pressure solver, the PV-coupling scheme, first-order methods for momentum, density, temperature, and k-ω turbulence model. The regenerator and pulse tube were initialized with gradients from hot to cold temperatures, while the cold HX was initialized with the cold temperature so that the simulations would reach quasi-steady state more rapidly than if initialized from room temperature. Mesh adaption utilized the magnitude of the velocity spatial gradient technique. The boundary layer along the wall was adapted for the initial time-step of all component walls except the moving piston face. Monitors were placed at each component junction to save files for the typically area-weighted averaged CFD data at each time step. Each cycle consisted of 800 individual time steps. The simulation was run for 30 cycles and most data is quasi-steady state, and thus these results are considered preliminary in nature.

RESULTS AND DISCUSSION

Important integral quantities of interest in this study are the phase shift between the pressure and mass flow and exergy flow at the junction of each component. The pressure and mass flow rates are plotted in Figures 2a and 2b for the inlet and outlet of the pulse tube, respectively.

Sage yields the phase shift between the mass flow rate and the pressure at each component, while a Fast-Fourier-Transform (FFT) is utilized to obtain the phase shift at each component using the monitor data for mass flow rates and pressure. These comparisons are shown in Figure 3.

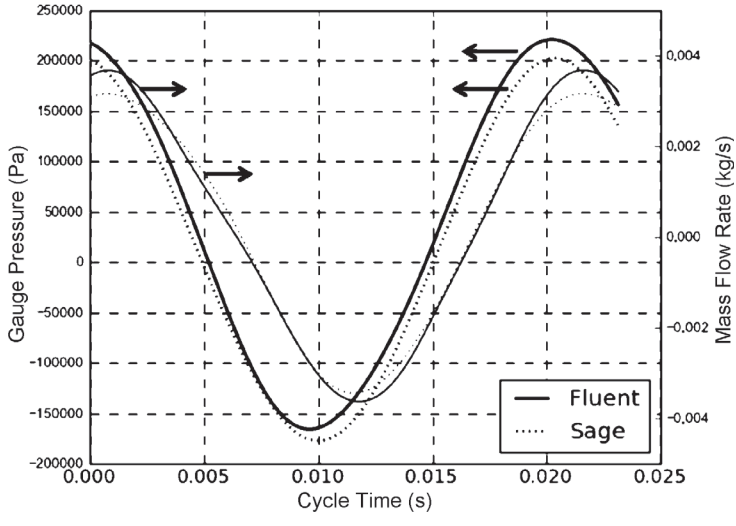

Figure 2a. Pulse tube entrance plots of the mass flow rates and pressures as a function cycle time as calculated by Sage and Fluent.

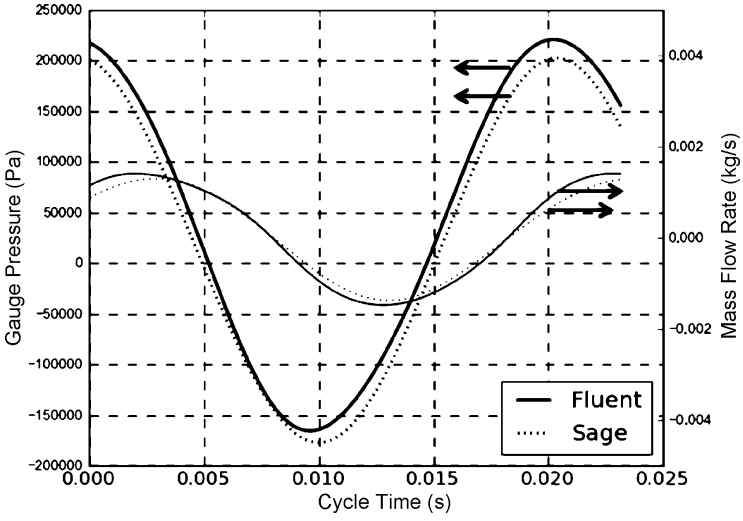

Figure 2b. Pulse tube exit plots of the mass flow rates and pressures as a function cycle time as calculated by Sage and Fluent.

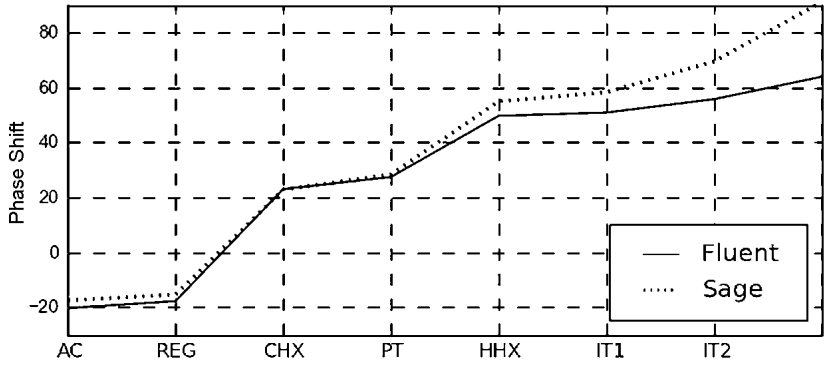

Figure 3. Phase shifts for aftercooler (AC), regenerator (REG), cold heat exchanger (CHX), pulse tube (PT), hot heat exchanger (HHX), inertance tube 1 & 2 (IT1 & IT2)

The Second Law of Thermodynamics and exergy analysis enables designers to understand the losses associated with the various components of the cryocooler (or any system). It should be recognized that in the context of PTCs, exergy analysis is another way of understanding the availability of the work left in the fluid at a component of a system. With the method one can track the locations, types and true magnitudes of waste and loss as the fluid traverses the system. The general specific exergy equation is given by,

$$e = (h - h_0) - T_0(s - s_0), \tag{1}$$

where h and s are the specific enthalpies and entropies, respectively, and the subscript '0' denotes those variables at the environmental reference state.

For cryocoolers cooling above about 30 K one can use the ideal gas law for the helium working fluid. For the ideal gas equation and a cryocooler component whose fluid has a constant specific heat, the specific exergy can be written as,

$$e = c_p(T - T_0) - c_p T_0 \ln\left(\frac{T}{T_0}\right) + RT_0 \ln\left(\frac{P}{P_0}\right), \tag{2}$$

where c_p is the specific heat of the gas, R is the ideal gas constant, T the temperature and P the pressure of the gas, and again the subscript '0' denotes the environmental reference state. The first

two terms are considered the thermal-based specific exergy, while the last term is the pressure-based specific exergy. These will be important for analysis of the PTC and general oscillating flow systems, since there are loss mechanisms in the components that are a combination of these two losses. With this technique we will be able to separate these loss mechanisms to identify which loss dominates at the various components and the trade-off that usually exists between the two components of exergy.

Due to the cyclic behavior of the PTC and general oscillating flow systems, the specific exergy must be integrated over the period (τ) of a cycle to obtain the flow exergy rate at each component monitor,

$$\dot{E} = \frac{1}{\tau}\int_0^{\tau} \dot{m}(t)e(t)dt. \tag{3}$$

With the above equation (where e(t) is defined as above, and $\dot{m}$ is the mass flow rate), as the gas temperature, pressure and mass flow rates change from component to component in the PTC, the exergy analysis tells how much exergy is transferred from one component to other components. The exergy balance over the surfaces of each component can be used to calculate the exergy destruction for that component. The irreversibilities can be tracked through the system to tell which components are most responsible for the losses, so the designers can focus on improving these components. Exergy analysis shows how modification in one component, like the heat exchanger, will affect the losses in other components and the system.

The irreversibilities from the CFD simulation of the regenerator is 28.4 W, the pulse tube is 30.2 W, the two inertance tubes is 14.2 W, with the exergy of cooling yielding 11.9 W. The second law efficiency can be calculated as,

$$\eta = \frac{exergy\ of\ production}{exergy\ in} = \frac{11.9}{89.42} = 13\%. \tag{4}$$

It should be pointed out that the irreversibility of the compressor is not included in the calculation.

The exergy should be calculated at each monitor using the CFD radial data as follows:

$$\dot{E}_x = \frac{1}{\tau}\int_0^{\tau}\int_0^{R} \dot{m}(r,x,t)e(r,x,t)2\pi r dr\, dt \tag{5}$$

Our calculation uses $\dot{m}(t)$ and $e(t)$ at an area weighted average monitor and integration is done at each monitor:

$$\dot{E}_x = \frac{1}{\tau}\int_0^{\tau} \dot{m}(x,t)e(x,t)dt \tag{6}$$

There could be errors in using this approximation in the exergy. Additionally the exergy should be calculated at all positions x to show how the exergy is destroyed through the axial position of each component, not just the interface between components as done in this study.

The temperatures on the sides of the cold heat exchanger next to the regenerator and pulse tube are shown in the left plot of Figure 4 for both the CFD and Sage models. The temperatures on the hot side of the pulse tube are shown in the right plot in Figure 4.

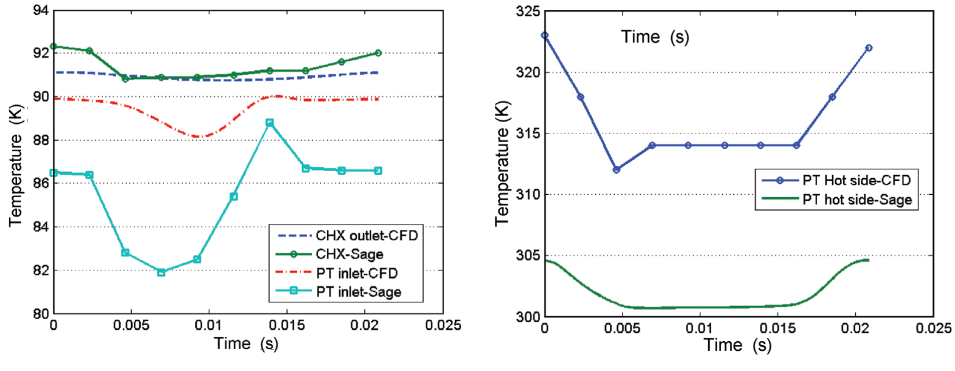

Figure 4. Temperatures (left) on the two ends of the cold heat exchanger (CHX) and (right) on the hot side of the pulse tube (PT)

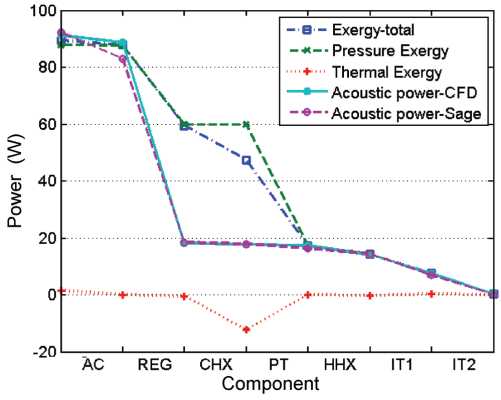

Figure 5. Exergy plots for aftercooler (AC), regenerator (REG), cold heat exchanger (CHX), pulse tube (PT), hot heat exchanger (HHX), inertance tube 1 & 2 (IT1 & IT2).

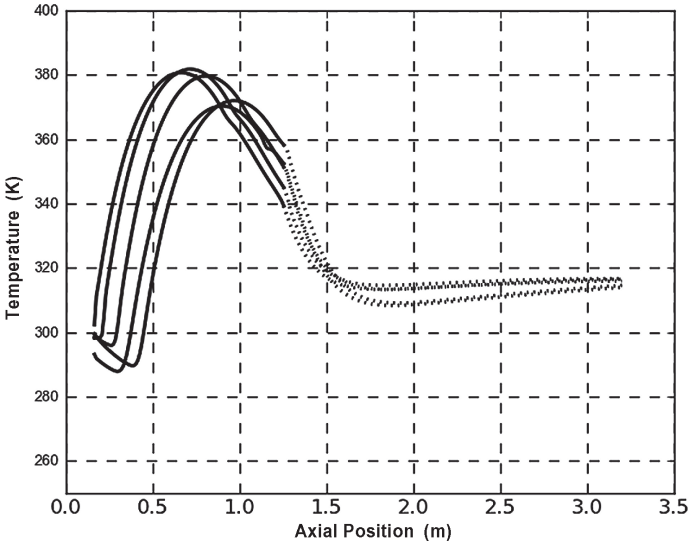

Figure 6. Temperature along the axis of the two inertance tubes (bold is IT1 and dotted is IT2) showing the temperature moving at different time steps.

The pressure exergy appears to not be as sensitive to a lack of conservation of mass for the CFD simulations, but the thermal exergy is and requires mass conservation better than 10^{-7} to be able to capture the effect of oscillating flow phenomena in PTRs. The exergy for the CFD and the acoustic power for both Sage and the CFD are shown for each component in Figure 5.

It has been noted in several coolers that the temperature in the inertance tube can get rather hot. This can be seen in Figure 6, which is a plot of the temperature along the axis of the two inertance tubes. The results given in this paper are all preliminary, as the temperature in the first inertance tube is still increasing. However, the results for phase shift, mass flow rate, and pressure amplitudes are very close to being converged and should be rather representative of a quasi-steady state simulation.

CONCLUSIONS

It has been shown that the preliminary results of the CFD simulation of a PTR compares well with Sage for phase shifts, mass flow rate, and pressures at the inlet and outlet of the pulse tube. Properly designed PTRs depend heavily on the control of the phase shift between mass flow rate

and pressure in the various components. The CFD simulation of the PTR included two inertance tubes for proper phase shifting between mass flow rate and pressure. The variation in temperature in the inertance tube that has been observed in experiments is observed in the CFD simulation as well. The exergy flow in the PTR at different component interface monitors was calculated using the CFD calculation. The thermal and pressure components of exergy were calculated at each monitor; therefore, the irreversibility of friction due to fluid flow and heat transfer due temperature can be separated.

REFERENCES

1. Radebaugh, R., "Development of the pulse tube refrigerator as efficient and reliable cryocoolers," *Proceedings of Institute of Refrigeration*, 2000, pp. 11-31.
2. Zhang, A., Chen, X., Wu, Y., Zhang, H. and Yang, K., "Study on 10 W/90K in-line pulse tube cryocooler," *Cryogenics,* vol. 52 no.12, December 2012, pp. 800-804.
3. Gedeon Associates, Sage, version 8.0.
4. ANSYS® Fluent, Release 14.5.7.
5. Dodson, C. *The comparison of CFD simulations and a first order numerical model of inertance tubes,* Master's Thesis, University of New Mexico, 2007.
6. Taylor, R., Nellis, G. and Klein, S., "Optimal Pulse-Tube Design Using Computational Fluid Dynamics," *Adv. in Cryogenic Engineering*, Vol. 53, Amer. Institute of Physics, Melville, NY (2008), pp. 1445-1453.
7. Cha, J.S., Ghiaasiaan, S.M., Desai, P.V., Harvey, and J.P., Kirkconnell, C.S., 'Multi-dimensional flow in pulse tube refrigerators," *Cryogenics*, 46, (2006), 658-665.
8. Chen, L., Zhang, Yu, Luo, E., Li, T., Wei, X., "CFD analysis of thermodynamic cycles in a pulse tube refrigerator," *Cryogenics*, 50, (2010), pp. 743-749.
9. Ashwin, T.R., Narasimham, G.S.V.L., and Jacob, S., "CFD analysis of high frequency miniature pulse tube refrigerators for space applications with thermal non-equilibrium model," *Applied Thermal Engineering*, 30, (2010), pp. 152-166.
10. Taylor, R.P., Nellis, G.F., Klein, S.A., Radebaugh, R., Lewis, M., Bradley, P., "Experimental validation of a pulse tube CFD model," *Adv. in Cryogenic Engineering*, Vol. 55, Amer. Institute of Physics, Melville, NY (2010), pp. 76-83.
11. Flake, B and Razani, A., "Modeling pulse tube cryocoolers with CFD," *Adv. in Cryogenic Engineering*, Vol. 49B, Amer. Institute of Physics, Melville, NY (2004), pp. 1493-1499.